Real-Time Dynamics and Phase Separation in a Holographic First-Order Phase Transition

Romuald A. Janik,[1,*] Jakub Jankowski,[2,†] and Hesam Soltanpanahi[3,‡]
[1]Institute of Physics, Jagiellonian University, Lojasiewicza 11, 30-348 Krakow, Poland
[2]Faculty of Physics, University of Warsaw, ulica Pasteura 5, 02-093 Warsaw, Poland
[3]School of Physics, Institute for Research in Fundamental Sciences (IPM), P.O. Box 19395-5531, Teheran 19538-33511, Iran
(Received 11 May 2017; revised manuscript received 23 October 2017; published 28 December 2017)

We study the fully nonlinear time evolution of a holographic system possessing a first order phase transition. The initial state is chosen in the spinodal region of the phase diagram, and it includes an inhomogeneous perturbation in one of the field theory directions. The final state of the time evolution shows a clear phase separation in the form of domain formation. The results indicate the existence of a very rich class of inhomogeneous black hole solutions.

DOI: 10.1103/PhysRevLett.119.261601

Introduction.—The concept of a phase transition is inherently an equilibrium one, and it is a theoretical challenge to formulate a framework in which it can be quantitatively studied in cases involving real time dynamics. Such a framework is offered by gauge-gravity duality, which was put forward about 20 years ago [1]. Gauge-gravity duality, also referred to as holography, is immanently related to field theory systems at strong coupling, and thus it is very useful to study nonperturbative physics—especially as, within this framework, one can work directly in the Minkowski signature and study real time dynamics. Recently, it has been demonstrated that well-known holographic first order phase transitions [2] are accompanied by an unstable spinodal region [3,4], in accordance with standard predictions [5]. The analysis was based on linear response theory; however, the true power of the dual gravitational approach is the possibility of investigating the fully nonlinear dynamic evolution of the system. Simultaneously with this Letter, this particular direction was recently undertaken in Ref. [6], where the spinodal region was studied in the holographic model of a phase transition. The final state of the time evolution was an inhomogeneous configuration approached at late times within the hydrodynamic approximation. A different setup of a homogeneous evolution was undertaken in Ref. [7]. Inhomogeneous, static configurations appearing in the context of a holographic first order phase transition were also recently studied in Ref. [8].

A natural question which arises is whether the final state will exhibit domains of the two coexisting phases with the same values of the free energy. The main result of this Letter is to demonstrate for the first time that, in the case of a three-dimensional nonconformal system with a holographic dual, such a phase separation will arise dynamically through a real time evolution from a perturbation in the spinodal region. The respective energy densities of the two components of the final state are very close to the corresponding energy densities determined at the critical temperature. This implies that the system undergoes a dynamical transition during which different regions of space become occupied with different phases of matter.

The holographic framework.—The holographic model we use is a bottom-up construction containing Einstein gravity coupled to a real, self-interacting scalar field. The action takes the standard form

$$S=\frac{1}{2\kappa_4^2}\int d^4x\sqrt{-g}\left[R-\frac{1}{2}(\partial\phi)^2-V(\phi)\right]+S_{\mathrm{GH}}+S_{\mathrm{ct}}, \tag{1}$$

where κ_4 is related to the four-dimensional Newton's constant $\kappa_4=\sqrt{8\pi G_4}$ and the self-interaction potential $V(\phi)$ is given below. We include the boundary terms in the form of Gibbons-Hawking S_{GH} [9] and holographic counterterms S_{ct} [10,11] contributions. We chose to work in $(3+1)$-dimensional bulk spacetime, which is dual to $(2+1)$-dimensional field theory, for the absence of conformal anomaly in odd dimensions. This, in turn, makes the expansions near the conformal boundary free from logarithms, which allows for the usage of Chebyshev spectral methods for numerical integration. The $V(\phi)$ potential is constructed so that the dual field theory undergoes an equilibrium first order phase transition. The specific choice that we use is

$$V(\phi)=-6\cosh\left(\frac{\phi}{\sqrt{3}}\right)+b_4\phi^4, \tag{2}$$

where $b_4=-0.2$. This functional form is dual to a relevant deformation of the boundary conformal field theory with an operator of conformal dimension $\Delta=2$. When $b_4=0$ the potential is that of $\mathcal{N}=2$ supergravity in $D=4$ after dimensional reduction from $D=11$ [12]. The physical scale, breaking conformal invariance, is set by the source of the operator and is chosen to be $\Lambda=1$. The equilibrium structure of this model is described in terms of dual black hole geometries characterized by specifying the horizon

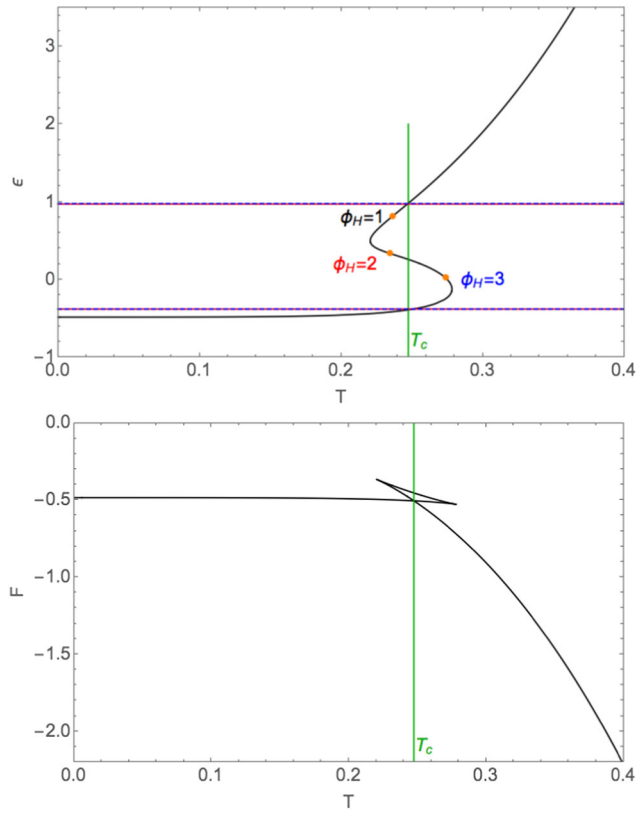

FIG. 1. (Upper panel) The temperature dependence of the holographic energy density. The vertical green line represents the transition temperature. Orange points represent sample chosen initial configurations for the time evolution. The horizontal lines show the domain energies in the final state (solid, cosine perturbation; dashed, Gauss perturbation). (Lower panel) Free energy as a function of temperature.

value of the scalar field, i.e., $\phi(z=1)=\phi_H$. The entropy and the free energy of the system are, in turn, given by the Bekenstein-Hawking formula and the on-shell value of the action (1), respectively. The corresponding thermodynamics reveals the appearance of a first order phase transition between different branches of black hole geometries as determined by the difference of the free energies. The order of the transition is established by a discontinuity of the first derivative of the free energy of the system. This effect is illustrated in the lower panel of Fig. 1. The value of the critical temperature is $T_c \simeq 0.246$ (in $\Lambda=1$ units). This transition is of a similar nature as the Hawking-Page transition in the case of anti–de Sitter (AdS) space [13,14] (an important difference, however, is that, in the current setup, all phases are of the black hole type). The equation of state (EOS) is displayed in the upper panel of Fig. 1 as a temperature dependence of the energy density. This EOS is similar to the five-dimensional gravity theory minimally coupled to a scalar field studied in Ref. [3,4], and the detailed analysis of the linearized dynamics proved, in accordance with the general lore, the existence of a spinodal region separating stable configurations [3,4].

Time dependent configurations.—To study the time evolution of the system, we adopt the following metric ansatz in the Eddington-Finkelstein (EF) coordinates:

$$ds^2 = -Adt^2 - \frac{2dtdz}{z^2} - 2Bdtdx + S^2(Gdx^2 + G^{-1}dy^2), \tag{3}$$

where all functions are x, t, and z dependent. We can take the initial state to lie in the spinodal region of the phase diagram and add an x-dependent perturbation to the S function. By the proper choice of the perturbing function,

$$\delta S(t,x,z) = S_0 z^2(1-z)^3 \cos(kx), \tag{4}$$

we can turn on a particular unstable mode or add a mixture of all modes,

$$\delta S(t,x,z) = S_0 z^2(1-z)^3 \exp[-w_0 \cos(\tilde{k}x)^2], \tag{5}$$

with different widths. By solving the time dependent Einstein-matter equations of motion with proper AdS boundary conditions at $z=0$, we determine the nonlinear evolution of the system. [In the EF coordinates, $A \sim 1/z^2 + O(1)$, $S \sim 1/z + O(1)$, $G \sim O(z)$, and $B \sim O(z)$ for $z \to 0$.] Using the procedure of holographic renormalization, we then read off the relevant observables like the energy density of the boundary theory from subleading terms in the near-boundary expansion [10,11].

The system is essentially studied in the microcanonical ensemble as the total energy density of the system is fixed throughout the evolution. The gravitational formulation of the problem is now given by a coupled set of nonlinear partial differential equations. We solve that problem numerically using the characteristic formulation of general relativity [15] along with spectral methods [16]. In the relevant spatial direction, we use periodic boundary conditions with spectral Fourier discretization. The remaining spatial direction is uncompactified.

Results.—Since, for this system, the energy density in equilibrium uniquely determines the temperature, we may deduce that the final state of evolution starting from the unstable spinodal branch necessarily has to be inhomogeneous. The physical expectation that the final state will consist of well separated phases at the phase transition temperature $T=T_c$ would manifest itself in the existence of spatial domains characterized by very flat energy density, the values of which should coincide with the energy densities of the two stable phases at $T=T_c$. The fact that such a configuration is attained dynamically even when starting from points on the spinodal branch with temperatures differing from T_c is far from trivial. That is the main result of this Letter.

To illustrate the effect of the appearance of different phases during the time evolution, we run the simulations for a number of initial configurations, covering a representative region of interest. Some of the configurations are marked with orange dots in Fig. 1. As was explained in the previous

section, we use two different shapes of perturbing function given in Eqs. (4) and (5) with different values for parameters. Particularly transparent results appear for the value of the momentum equal to $k = 1/6$ and $\tilde{k} = 1/12$, with $w_0 = 10$, and we have chosen to present those in this Letter. The amplitudes of the perturbations are in the range $S_0 = 0.1$–0.5.

The first point of interest is a large black hole configuration with a temperature below T_c, but still on the stable branch, e.g., with $\phi_H = 1$. The linear analysis shows no instability of that configuration. However, one could still expect a nonlinear instability due to overcooling. In our simulations we found, however, no evidence of that within the considered framework.

The second considered point, with $\phi_H = 2$, is placed deep in the unstable region. The temporal and spatial dependence of the energy density is shown in the upper panel of Fig. 2. The initially small Gaussian perturbation grows with time, and after around 400 units of simulation time starts settling down to an inhomogeneous final state. The maximum and the minimum energy of this state, marked as horizontal solid lines in Fig. 1, approach to less than 1% the energy densities determined by the transition temperature. Pronounced flat regions of constant energy density are apparent at late stages of the evolution. It is clearly visible that in the final state different parts of the system are occupied by the different phases, joined by a domain wall.

The third considered configuration, with $\phi_H = 3$, lies close to the end of the spinodal region. The time dependence of the energy density in this case is displayed in the lower panel of Fig. 2. The perturbation added is a single cosine mode. In this case, after about 150 units of simulation time, the configuration settles down to an inhomogeneous final state. The maximum and minimum energy densities of this final state are marked with horizontal dashed lines in Fig. 1. Similarly to the previous configuration, the extrema of energy density reach the corresponding densities determined at the transition temperature $T = T_c$. However, due to the fact that the initial energy density is smaller than the energy density of a configuration with $\phi_H = 2$, we observe a smaller region of the high-energy phase in the final state.

To summarize the above results, we display the final state energy density as a function of x in Fig. 3 for both unstable initial configurations. The Hawking temperature of the final state geometry is constant and equal to the critical temperature T_c. From the field theory perspective, this is a clear demonstration of the coexistence phenomenon, where an inhomogeneous state has a constant temperature. Different regions of space are occupied by different phases connected by domain walls. Despite the fact that, in both cases, the final state is rather universal, the time evolution is substantially different. The great novelty of our approach is that details of dynamical formation of domains of different phases can be studied quantitatively. In order to do so, it is convenient to introduce the following observable:

$$A_\epsilon = \frac{1}{12\pi}\int_{\epsilon>\epsilon_0} \epsilon(t,x)dx, \tag{6}$$

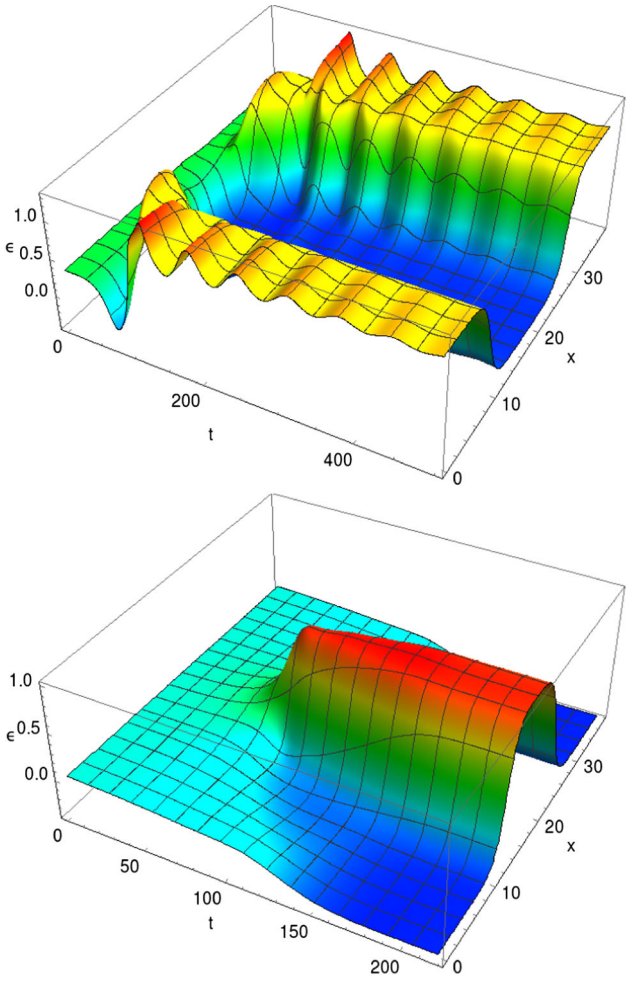

FIG. 2. The energy density as a function of time for the initial configuration in the spinodal region. (Upper panel) $\phi_H = 2$, Gaussian perturbation. (Lower panel) $\phi_H = 3$, cosine perturbation.

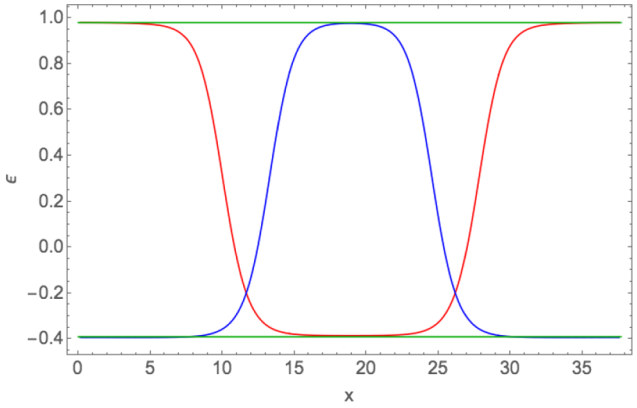

FIG. 3. The final state energy density for different initial configurations: $\phi_H = 2$ (the red line) and $\phi_H = 3$ (the blue line). The horizontal green lines represent the energy densities at the critical temperature in isotropic solutions.

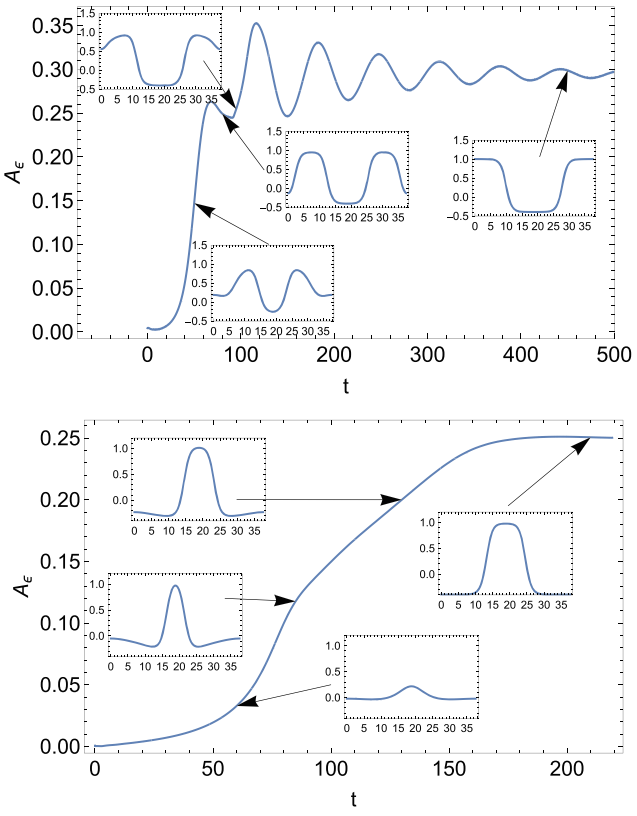

FIG. 4. The time evolution of the observable A_ϵ defined in Eq. (6). (Upper panel) Configuration starting from $\phi_H = 2$. (Lower panel) Configuration starting from $\phi_H = 3$. (Insets) Profiles of the energy density at given instants. See the discussion in the text.

where ϵ_0 is the mean energy of the system at $t = t_0$. The above quantity essentially measures the amount of energy *above* the mean energy stored in the system at $t = t_0$. As is clearly seen in Fig. 4, in both considered cases the details of dynamics are different. (These differences stem from the different forms of the perturbation employed by us at $\phi_H = 2$ and $\phi_H = 3$.) For the configuration with $\phi_H = 2$ the initial perturbation develops into two bubbles which subsequently move away from the center and then violently coalesce and merge into one final domain. For this reason, the final state is approached with large, damped oscillations. By contrast, the configuration with $\phi_H = 3$ displays less violent evolution. We can identify three stages of evolution in that case. First is an exponential growth of the instability that takes place roughly until the maximum energy reaches the equilibrium energy density. The second stage displays a linear increase of the bubbles' width with a fixed height to form an extended region. The system finally saturates in the third stage, with small oscillations for late times. In both cases the complicated dynamics is a consequence of the nonlinear nature of dual Einstein equations, and it would be extremely difficult to study using conventional field theory techniques. In future work we intend to analyze in more detail both of these

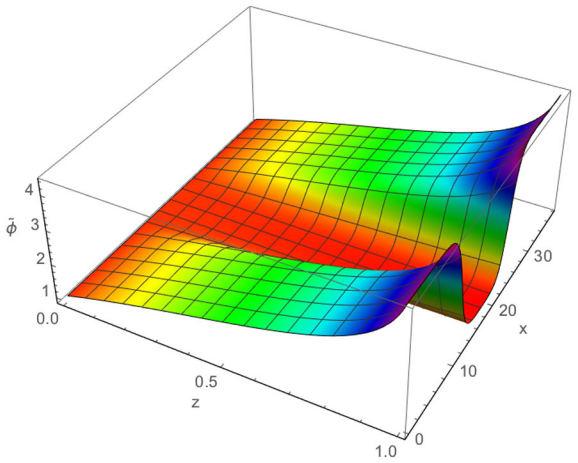

FIG. 5. The final configuration of the scalar field $\tilde{\phi}(x, z) = \phi(x, z)/z$ extending to the inhomogeneous horizon at $z = 1$ for the solution starting from $\phi_H = 3$.

phenomena: the collision of fully formed domains of equilibrium phases and the details of the dynamics of bubble growth.

Discussion.—In this Letter we demonstrated for the first time the existence of a phase separation effect at the transition temperature of a first order phase transition in the context of holographic models. The chosen setup was a bottom-up holographic construction designed to exhibit an equilibrium first order phase transition.

The full nonlinear time evolution of a perturbed configuration with a spinodal instability ended in an inhomogeneous state composed of domains of different stable phases as determined at the transition temperature fixed by the equality of free energies. The dual gravitational configuration is a black hole with an inhomogeneous horizon. However, in contrast to the results of Ref. [6], the geometries obtained here correspond to domains of specific thermodynamic phases with very mild spatial dependence separated by relatively narrow domain walls. On the gravitational side, this means that the bulk geometry consists of two distinct types of black holes, characterized, e.g., by the value of the scalar field on the horizon smoothly connected by interpolating domain walls (see Fig. 5 for a sample configuration of the scalar field in the bulk). Despite the inhomogeneity, the Hawking temperature is constant on the horizon. From the field theory interpretation, we expected to have an immense moduli space of geometries which correspond to different configurations of phase domains coming from different seed perturbations. Indeed, we found also solutions with multiple potential domains which, however, were of a size on the order of the domain wall width and thus were more similar to the solutions of Ref. [6]. It is clear that, with an appropriately large transverse spatial extent of the simulation, one can explicitly construct solutions with multiple domains. We intend to investigate this in the future.

We also demonstrated that large black holes with temperatures below the critical value are stable against the perturbations that we tried. This indicates that, in the holographic description, we may naturally expect an overcooled phase which only starts to nucleate once it has dynamically moved into the spinodal branch.

There are numerous directions for further research. Apart from studying the space of domain geometries mentioned earlier, it would be very interesting to investigate in detail the various temporal regimes which can be seen in Fig. 4 and study the dynamics of the phase domains. Naturally, it would be good to investigate extensions to other dimensions as well as to ultimately relax any symmetry assumptions. An additional bonus of the present setup is the appearance of configurations breaking translation invariance without specifying explicit inhomogeneous sources. In other words, the final state solutions spontaneously break translational invariance. This opens the possibility of applications in the context of condensed matter physics [17,18].

We would like to thank Z. Bajnok for the extensive discussions and collaboration in the initial stage of the project. R. J. was supported by NCN Grant No. 2012/06/A/ST2/00396. J. J. was supported by NCN Grant No. UMO-2016/23/D/ST2/03125. J. J. and H. S. would like to thank the theory division at CERN, Wigner Institute, and Jagiellonian University, where a part of this research was carried out. H. S. would like to thank Witwatersrand University, where part of this research was done. R. J. would like to thank the Galileo Galilei Institute for Theoretical Physics for its hospitality and the INFN for the partial support during the completion of this work.

*romuald@th.if.uj.edu.pl
†jjankowski@fuw.edu.pl
‡hsoltan@ipm.ir

[1] J. M. Maldacena, The large N limit of superconformal field theories and supergravity, Adv. Theor. Math. Phys. **2**, 231 (1998).
[2] S. S. Gubser and A. Nellore, Mimicking the QCD equation of state with a dual black hole, Phys. Rev. D **78**, 086007 (2008).
[3] R. A. Janik, J. Jankowski, and H. Soltanpanahi, Nonequilibrium Dynamics and Phase Transitions in Holographic Models, Phys. Rev. Lett. **117**, 091603 (2016).
[4] R. A. Janik, J. Jankowski, and H. Soltanpanahi, Quasinormal modes and the phase structure of strongly coupled matter, J. High Energy Phys. 06 (2016) 047.
[5] P. Chomaz, M. Colonna, and J. Randrup, Nuclear spinodal fragmentation, Phys. Rep. **389**, 263 (2004).
[6] M. Attems, Y. Bea, J. Casalderrey-Solana, D. Mateos, M. Triana, and M. Zilhao, Phase transitions, inhomogeneous horizons and second-order hydrodynamics, J. High Energy Phys. 06 (2017) 129.
[7] U. Gürsoy, A. Jansen, and W. van der Schee, New dynamical instability in asymptotically anti–de Sitter spacetime, Phys. Rev. D **94**, 061901 (2016).
[8] O. J. C. Dias, J. E. Santos, and B. Way, Localised and nonuniform thermal states of super-Yang-Mills on a circle, J. High Energy Phys. 06 (2017) 029.
[9] G. W. Gibbons and S. W. Hawking, Action integrals and partition functions in quantum gravity, Phys. Rev. D **15**, 2752 (1977).
[10] K. Skenderis, Lecture notes on holographic renormalization, Classical Quantum Gravity **19**, 5849 (2002).
[11] H. Elvang and M. Hadjiantonis, A practical approach to the Hamilton-Jacobi formulation of holographic renormalization, J. High Energy Phys. 06 (2016) 046.
[12] M. J. Duff and J. T. Liu, Anti–de Sitter black holes in gauged $N = 8$ supergravity, Nucl. Phys. **B554**, 237 (1999).
[13] S. W. Hawking and D. N. Page, Thermodynamics of black holes in anti–de Sitter space, Commun. Math. Phys. **87**, 577 (1983).
[14] E. Witten, Anti–de Sitter space, thermal phase transition, and confinement in gauge theories, Adv. Theor. Math. Phys. **2**, 505 (1998).
[15] P. M. Chesler and L. G. Yaffe, Numerical solution of gravitational dynamics in asymptotically anti–de Sitter spacetimes, J. High Energy Phys. 07 (2014) 086.
[16] P. Grandclement and J. Novak, Spectral methods for numerical relativity, Living Rev. Relativity **12**, 1 (2009).
[17] G. T. Horowitz, J. E. Santos, and D. Tong, Optical conductivity with holographic lattices, J. High Energy Phys. 07 (2012) 168.
[18] A. Donos and J. P. Gauntlett, Holographic Q-lattices, J. High Energy Phys. 04 (2014) 040.